

## Size-induced diffuse phase transition in the nanocrystalline ferroelectric $\text{PbTiO}_3$

Soma Chattopadhyay, Pushan Ayyub, V. R. Palkar, and Manu Multani

*Materials Research Group, Tata Institute of Fundamental Research, Homi Bhabha Road, Bombay 400 005, India*

(Received 24 May 1995)

We report a detailed study of the size dependence of the ferroelectric transition in an ensemble of  $\text{PbTiO}_3$  nanoparticles produced by coprecipitation. The phase transition was monitored by dielectric measurements, variable temperature x-ray diffraction, and differential scanning calorimetry (DSC). Size effects were found to become important only below  $\approx 100$  nm (coherently diffracting x-ray domain size). The tetragonal distortion of the unit cell (which is related to the spontaneous polarization) decreases exponentially with size and vanishes at 7 nm. The  $T_c$  decreases gradually but the transition becomes increasingly diffuse with a decrease in the size from 80 to 30 nm, below which there is no peak in the dielectric constant or the heat flow (DSC), though ferroelectric ordering probably persists down to  $\approx 7$  nm.

### I. INTRODUCTION

Investigations of the effect of particle size on the phase transition in ferroelectric systems date back to the 1950s, when Känzig and co-workers studied fine particles of order-disorder (e.g.,  $\text{KH}_2\text{PO}_4$ ) as well as displacive (e.g.,  $\text{BaTiO}_3$ ) types of ferroelectrics.<sup>1,2</sup> The earlier work (with some exceptions) involved grain sizes between 1–5  $\mu\text{m}$ , since it was difficult to synthesize finer particles with a controlled particle size and size distribution. For sintered samples with high density and minimum nonstoichiometry, it was found<sup>3–5</sup> that with a decrease in grain size in the 1–5  $\mu\text{m}$  range: (i) there is a decrease in the peak dielectric constant  $\epsilon_{\text{max}}$ , (ii) the peak in the  $\epsilon$ - $T$  curve becomes broader, and (iii) the ferroelectric transition temperature ( $T_c$ ) goes up. But with the availability of more advanced chemical techniques (sol-gel, hydrosol, aerosol, microemulsion, etc.), as well as spray-type and thin-film type techniques for the preparation of homogeneous ultrafine ceramic particles, it is now established that the ferroelectric  $T_c$  decreases with decreasing particle size in the submicron range. The study of size effects in ferroelectric systems have lately become very important because of their potential applications, especially as nonvolatile memory elements.

Kanata *et al.*<sup>6</sup> have shown that in fine particles of  $\text{BaTiO}_3$  with grain size  $< 20$   $\mu\text{m}$ , the  $T_c$  (at which temperature the crystal symmetry changes from tetragonal to cubic) decreases with decreasing particle size. They attributed this shift to superparaelectricity and pointed out the importance of the internal stresses that develop spontaneously in small grains. Uchino *et al.*<sup>7</sup> made a more detailed study of the variation of the tetragonal distortion ( $c/a$ ) with particle size in  $\text{BaTiO}_3$  and, having identified the  $T_c$  as that temperature at which  $c/a \rightarrow 1$ , estimated the critical size for the existence of ferroelectricity ( $d_{\text{crit}}$ ) to be 120 nm. However, they had not made dielectric or other measurements to support the value of  $T_c$  determined from structure data at different temperatures.

Here we report a study of the ferroelectric transition in nanocrystalline  $\text{PbTiO}_3$ .  $\text{PbTiO}_3$  is a classical displacive ferroelectric with excellent dielectric, pyroelectric, and piezo-

electric properties. It has a tetragonal perovskite structure ( $a = 0.3899$  nm,  $c = 0.4153$  nm) at room temperature, and transforms to a cubic paraelectric phase ( $a = c = 0.396$  nm) above  $T_c = 763$  K. Ishikawa *et al.*<sup>8</sup> earlier prepared  $\text{PbTiO}_3$  fine particles by an alkoxide method and made a Raman study of samples with different average particle size as a function of temperature. The ferroelectric  $T_c$  was indirectly measured as the temperature at which the frequency ( $\omega_s$ ) of the soft  $E(1TO)$  mode ( $\omega_s \rightarrow 0$  as  $T \rightarrow T_c$ ) vanishes.<sup>9</sup>  $T_c$  was again found to decrease with decreasing particle size with  $d_{\text{crit}} = 12.6$  nm. Zhong *et al.*<sup>10</sup> made further Raman-scattering measurements on  $\text{PbTiO}_3$  at room temperature for particles of different average sizes and the  $\omega_s$  was found to shift towards lower frequencies with decreasing size, which was taken to imply a lowering of  $T_c$  with size. The  $T_c$  obtained from differential scanning calorimetry (DSC) was also found to obey a similar trend.

There appears to be no definitive report of the measurement and interpretation of the dielectric response function in nanocrystalline ferroelectric systems. A difficulty with carrying out this important measurement in  $\text{PbTiO}_3$  relates to the preparation of properly compacted samples, since a large strain is developed when it undergoes the tetragonal to cubic structural transition at the  $T_c$ , which often leads to the pellet crumbling. It is also important to attempt to correlate the  $T_c$  determined from different techniques such as dielectric, thermal, and structural ( $c/a$ ) measurements. Such comparative studies are obviously essential for a complete understanding of finite-size effects on the phase transition in nanocrystalline ferroelectrics. Further, it is necessary to reconcile the different “particle sizes” that one obtains from different techniques and understand the effect of the distribution in the particle size—a disturbing but unavoidable aspect of the problem.

We have prepared ultrafine particles of  $\text{PbTiO}_3$  (down to  $\approx 20$  nm) by coprecipitation—which is simpler than sol-gel based techniques. The average particle size was measured by x-ray diffraction (XRD) line broadening and compared with specific surface area and scanning electron microscope (SEM) observations. To obtain a complete and consistent understanding, the phase transition in the small solid ensemble was studied by three complementary techniques: measurement of the dielectric response vs temperature, measurement

of the temperature dependence of the tetragonal or ferroelectric distortion ( $c/a$ ), and DSC. XRD measurements were also made at temperatures down to 15 K to confirm that the large change observed in  $c/a$  is inherently a particle size effect. Finally, a qualitative attempt is made to understand the mechanism of the nature of the phase transition in nanocrystalline ferroelectrics.

## II. EXPERIMENTAL

### A. Synthesis of nanocrystalline PbTiO<sub>3</sub>

Ultrafine PbTiO<sub>3</sub> was prepared by coprecipitation from a stoichiometric mixture of Pb(NO<sub>3</sub>)<sub>2</sub> and TiCl<sub>4</sub>. TiCl<sub>4</sub> solution (in HCl) was first converted to Ti(OH)<sub>4</sub> by adding NH<sub>4</sub>OH, followed by concentrated HNO<sub>3</sub> to convert it to soluble Ti(NO<sub>3</sub>)<sub>4</sub>. The NH<sub>4</sub>NO<sub>3</sub> formed during reaction helps to prevent subsequent formation of insoluble PbCl<sub>2</sub>. An aqueous solution of Pb(NO<sub>3</sub>)<sub>2</sub> was added to the above before pouring the mixture into NH<sub>4</sub>OH solution. Care was taken to maintain a pH of 10.5 during the coprecipitation of Pb and Ti as hydroxides. The precipitate was filtered and washed with deionized water until the pH of the washing liquid was reduced to 7. It was then dried, crushed and heated at 150 °C for 1 h. This precursor material was subjected to thermogravimetric analysis (TGA) and the formation temperature for PbTiO<sub>3</sub> was thereby found to be  $\approx 450$  °C. The dry precursor was calcined at various temperatures between 460 and 850 °C (for 1 h at each temperature) to obtain PbTiO<sub>3</sub> particles with different average sizes (between 20 and 200 nm). Bulk PbTiO<sub>3</sub> (micron-sized particles) was obtained by heating the same precursor at 850 °C for 12 h. To avoid Pb-loss during calcination, all the samples were heated in an ambient of PbO. This was achieved by placing a mixture of PbO and yttria-stabilized zirconia in an alumina crucible in which was placed a smaller alumina crucible containing the pelletized sample. The larger crucible was covered with an alumina lid.

Chemical phase analysis was done from powder XRD measurements using a Jeol JDX 8030 instrument with a typical scan speed of 0.3° min<sup>-1</sup>. All the samples prepared were perfectly single phase to XRD. Neither could any segregated minority phases be located through energy dispersive x-ray analysis. The lattice constants  $a$  and  $c$  were calculated from the (100) and (001) reflections, respectively.

### B. Particle size measurement

The coherently diffracting domain size ( $d_{\text{XRD}}$ ) was calculated from the full width at half maximum (FWHM) of the (111) diffraction peak using the Scherrer equation which assumes the small crystallite size to be the only case of line broadening:<sup>11</sup>

$$d_{\text{XRD}} = K\lambda / \beta(\theta) \cos\theta \quad (1)$$

where  $\lambda$  is the x-ray wavelength,  $\beta(\theta)$  is the FWHM of the diffraction line,  $\theta$  is the angle of diffraction, and the constant  $K \approx 1$ . The contribution from instrumental broadening was removed by subtracting the FWHM of the (111) line in well-annealed, bulk PbTiO<sub>3</sub> ( $d \geq 3 \mu\text{m}$ ). If  $B$  and  $b$  are the measured FWHM, of equivalent diffraction lines in the specimen

and the reference (bulk sample), respectively, the FWHM of the true diffraction profile will be given by<sup>12</sup>

$$\beta^2 = B^2 - b^2 \quad (\text{for a Gaussian line shape}), \quad (2a)$$

$$\beta = B - b \quad (\text{for a Cauchy line shape}). \quad (2b)$$

Since the actual profiles are neither purely Gaussian nor purely Cauchy, we have used the approximate relation:<sup>13</sup>

$$\beta = B - b^2/B. \quad (3)$$

Before measuring the FWHM, the contribution due to the  $K\alpha_2$  radiation was removed from the spectra by the modified Rachinger method.<sup>14</sup>

The equivalent spherical diameter or ESD ( $d_{\text{BET}}$ ) of the particles was determined from the specific surface area measured by the Brunauer-Emmet-Teller (gas adsorption) technique<sup>15</sup> using a Quantachrome Quantasorb Jr. instrument after degassing the samples at 150 °C. The size, shape, and size distribution were also studied from micrographs obtained from a Jeol JSM-840 scanning electron microscope (SEM).

### C. Measurement of $T_c$

Dielectric measurements were made on pressed pellets of 1.0 cm diameter and 0.2 cm thickness. For this, the precursor material was pelletized and calcined at different temperatures. The pellet surfaces were cleaned in fumes of trichloroethylene before being coated with air-drying conducting silver paste and cured at 400 °C for 1 h. The capacitance and the dielectric loss factor ( $\tan\delta$ ) were measured at three frequencies (200 kHz, 500 kHz, and 1 MHz) using a Hewlett-Packard 4277A impedance analyzer. The heating rate was 5 °C min<sup>-1</sup> up to 350 °C and 2 °C min<sup>-1</sup> between 350 and 600 °C. Temperature was measured to  $\pm 1$  °C accuracy using a Pt/Pt-Rh thermocouple. The ferroelectric  $T_c$  was identified as the temperature corresponding to the maximum value of the real part of the dielectric response function.

The tetragonal distortion ( $c/a$ ) in the ferroelectric phase scales with the spontaneous polarization (which is the order parameter) in this class of compounds. The temperature dependence of  $c/a$  was determined from XRD spectra in the 15–723 K range using a Siemens D-500 x-ray diffractometer coupled with either a Buehler high-temperature camera or an Anton-Paar He-TTK closed cycle refrigerator. Diffraction patterns were recorded after stabilizing at each temperature for at least 15 min. The  $T_c$  was identified as the temperature at which  $c/a \rightarrow 1$ .

TABLE I. Variation of the ferroelectric transition temperature ( $T_c$ ) and diffuseness coefficient ( $\gamma$ ) with particle size in PbTiO<sub>3</sub>.

XRD size ( $d_{\text{XRD}}$ ) (nm)	BET size ( $d_{\text{BET}}$ ) (nm)	$T_c$ (dielectric) (°C)	$T_c$ (DSC) (°C)	Diffuseness ( $\gamma$ )
81	3137	506	502.5	1.00
57	768	500	493.3	1.17
39	186	498	490.5	1.214
36	148	496	489.8	1.317
31	92	488	486.8	1.503
26	74	No peak	No peak	

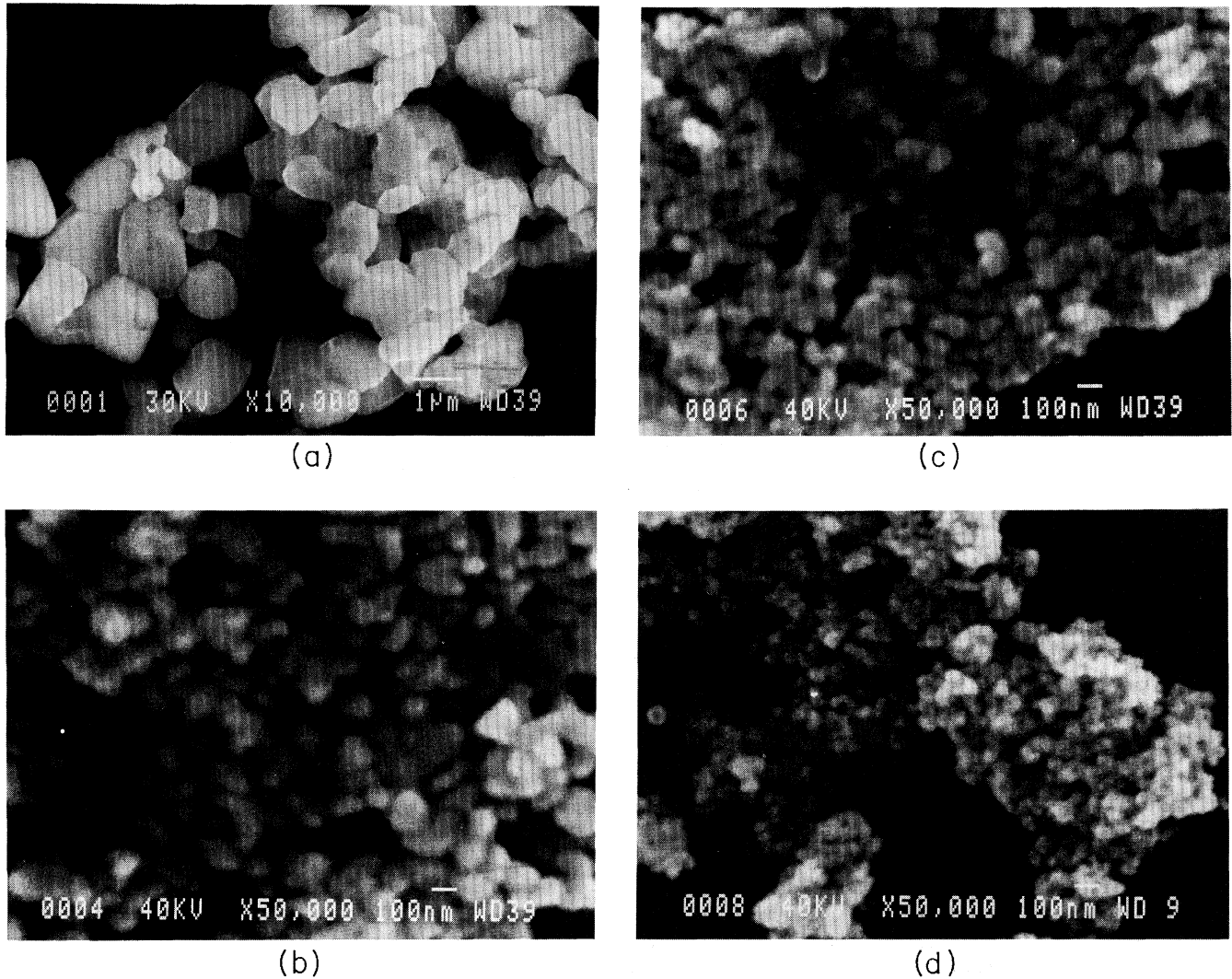


FIG. 1. SEM images of (a) bulk (Johnson Matthey, Puratronic grade)  $\text{PbTiO}_3$ , ESD =  $1.77 \mu\text{m}$  ( $\times 10\,000$ ), and three typical samples of  $\text{PbTiO}_3$  produced by coprecipitation with (b) ESD =  $111 \text{ nm}$  ( $\times 50\,000$ ), (c) ESD =  $83.5 \text{ nm}$  ( $\times 50\,000$ ), and (d) ESD =  $43.5 \text{ nm}$  ( $\times 50\,000$ ).

The  $T_c$  was also determined from differential scanning calorimetry performed in the range of  $50\text{--}550^\circ\text{C}$  using a Perkin-Elmer DSC-7 power compensation type calorimeter. The powder samples (typically  $\approx 20 \text{ mg}$ ) were encapsulated in aluminum crucibles and scanned at a rate of  $5^\circ\text{C min}^{-1}$ .

### III. RESULTS

#### A. Structural and thermal data

SEM images for a few of the samples with different average sizes are shown in Fig. 1. The  $\text{PbTiO}_3$  particles prepared by coprecipitation are shown to have a narrow size distribution. The ESD determined from surface area measurements compares very well with the average particle size seen in the SEM pictures. However,  $d_{\text{XRD}}$  is consistently much smaller than  $d_{\text{BET}}$  (see Table I), which is only to be

expected since each particle could consist of several coherently diffracting domains. It is also clear from Table I that the larger the particle, the greater is the number of domains it contains. This occurs due to thermally activated growth of particles by aggregation. Since ferroelectric phenomena in perovskites and other *displacive* systems are controlled by lattice vibrational mechanisms, we expect that of the three “sizes” that we have measured, the one most relevant to the problem is  $d_{\text{XRD}}$ . Henceforth—unless otherwise specified—all references to “particle size” should be taken to imply  $d_{\text{XRD}}$ .

Figure 2 shows the variation of the lattice constants  $a$  and  $c$  with particle size at room temperature. The unit cell does not change its dimensions down to  $\approx 150 \text{ nm}$ , below which  $c$  decreases and  $a$  increases with decreasing size. The resulting reduction in the tetragonal distortion  $c/a$  becomes especially rapid when the size goes below about  $60 \text{ nm}$  (Fig.

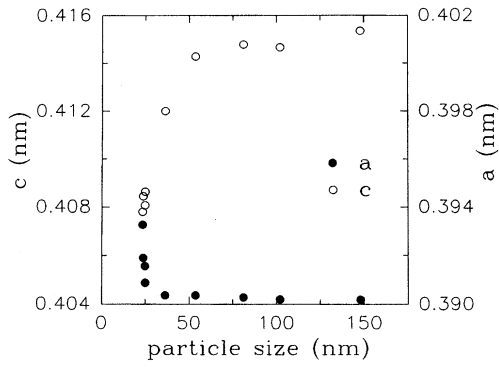


FIG. 2. Particle size dependence of the lattice constants  $a$  (filled circles) and  $c$  (empty circles) in  $\text{PbTiO}_3$  at room temperature.

3). This, in turn, implies that there is a decrease in the spontaneous polarization ( $P_S$ ) in nanocrystalline  $\text{PbTiO}_3$ . A least-squares fitting of a  $(1 - e^{-x})$  type curve to the data and a subsequent determination of the ferroelectric critical size is discussed in Sec. IV A. To ascertain whether (a) the low value of  $c/a$  (and hence  $P_S$ ) in nanoparticles is intrinsically a size effect, or (b)  $c/a$  simply has a different temperature dependence in fine particles and approaches the “bulk” value at low temperatures, we measured  $c/a$  in samples with different average size over a wide range of temperatures. Figure 4 shows that the size-induced reduction in the value of  $c/a$  does persist even at low temperature.

More importantly, the variable temperature XRD data (15–823 K) tell us about the size dependence of the “structural”  $T_C$ . We define this as the temperature at which the (001)-(100) and the (002)-(200) line splittings disappear, i.e., the ferroelectric distortion,  $c/a \rightarrow 1$ . The structural  $T_C$  was found to decrease with decreasing particle size (Fig. 4).

Figure 5 shows the heat flow vs temperature (DSC trace) for  $\text{PbTiO}_3$  particles of different size. The “thermal”  $T_C$  was identified with the temperature of the peak in the heat flow associated with the disappearance of the ferroelectric order. For each sample corresponding to a particular particle size, at least three DSC scans were made (on fresh samples each time). We observed—as did Zhong *et al.*<sup>10</sup>—that the scatter in the measured values of  $T_C$  was larger (but  $\Delta T_C$  was always

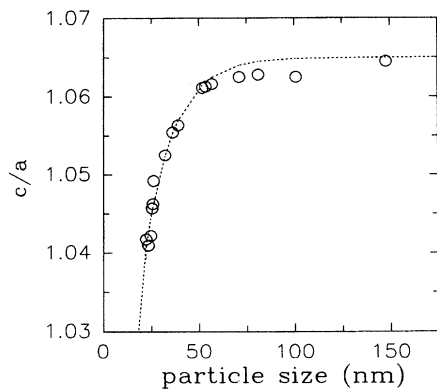


FIG. 3. Variation of the tetragonal distortion  $c/a$  with particle size. The dashed line is an empirical least-squares fit to Eq. (4).

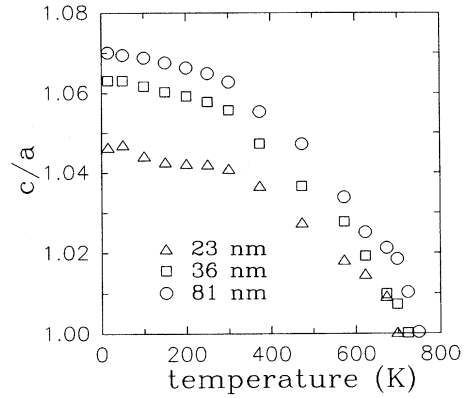


FIG. 4. Temperature dependence of the tetragonal distortion ( $c/a$ ) for  $\text{PbTiO}_3$  samples with different average sizes.

less than  $\pm 2$  °C) in smaller-sized samples. The  $T_C$  was again found to decrease with a decrease in particle size (Table I) and there was also a progressive increase in the peak width. For particles with  $d_{\text{XRD}} < 30$  nm, no transition peaks were observed in the DSC trace.

## B. Dielectric data

The temperature dependence of the dielectric response function ( $\epsilon$ ) and the dielectric loss ( $\tan \delta$ ) were measured between room temperature and 600 °C at three different frequencies. At least three pellets were scanned for each sample corresponding to a particular size. Again,  $\Delta T_C (\leq \pm 3$  °C) was found to increase with decreasing particle size. We find (Fig. 6) that with a decrease in the particle size,  $T_C$  decreases,  $\epsilon_{\text{max}}$  decreases and the peaks become increasingly broader. For samples with a size of 26 nm and below, no peaks were observed in the  $\epsilon$  vs  $T$  curves. The nature of the “dielectric” and the “thermal” transitions therefore show qualitatively similar changes with a reduction in the particle size.

We see (Fig. 7) that in bulk  $\text{PbTiO}_3$  ( $d_{\text{XRD}} \geq 60$  nm), a decrease in frequency leads to an increase in the  $\epsilon_{\text{max}}$ , but the ferroelectric  $T_C$  remains constant at  $\approx 500$  °C. Also, in bulk  $\text{PbTiO}_3$ , the peak in the  $\tan \delta$  vs  $T$  curve occurs at

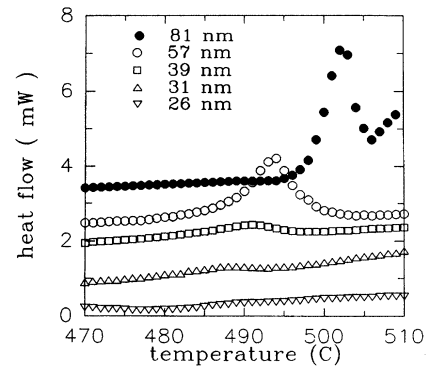


FIG. 5. DSC data (in the region of the ferroelectric transition) for  $\text{PbTiO}_3$  particles with different average sizes. The measurements were made in the temperature increasing mode with a scan rate of  $5$  °C  $\text{min}^{-1}$ .

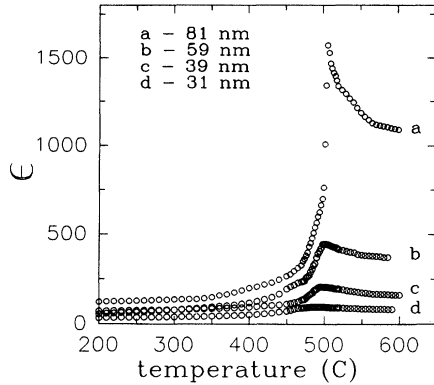


FIG. 6. Temperature dependence of the dielectric function  $\epsilon$  for  $\text{PbTiO}_3$  samples with different average size (all measured at 1 MHz).

474 °C, i.e., it precedes the peak in  $\epsilon$ . The dielectric loss is rather high in the nanocrystalline samples because—for obvious reasons—the measurements were made on unsintered pellets. In smaller particles of  $\text{PbTiO}_3$  ( $d_{\text{XRD}}=31$  nm), however, we find that the  $T_c$  moves up with an increase in frequency from 476 °C at 500 kHz to 488 °C at 1 MHz (Fig. 8), but there is no significant difference in the value of  $T_c$  measured at 200 and 500 kHz. A similar behavior was also observed in the other samples with low particle size. The shallow hump in  $\tan\delta$  that is observed for each of the frequencies, also moves up in temperature with a decrease in frequency. Note also that the temperature interval between the maxima in  $\tan\delta$  and  $\epsilon$  (for a particular frequency) is larger in finer particles. These properties are typical of materials with a diffused phase transition, as discussed in the next section.

#### IV. DISCUSSIONS

##### A. Size-induced structural distortion

One of the most significant effects of size reduction is a progressive increase in the symmetry of the crystal structure, reflected by a monotonic decrease in the tetragonal distortion

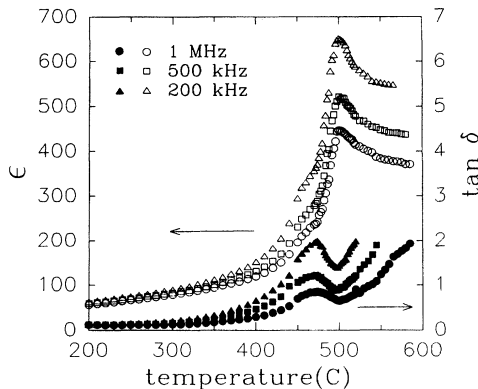


FIG. 7. Temperature dependence of  $\epsilon$  (empty symbols) and  $\tan\delta$  (filled symbols) in  $\text{PbTiO}_3$  with  $d_{\text{XRD}}=57$  nm for three different frequencies (200 kHz, 500 kHz, and 1 MHz).

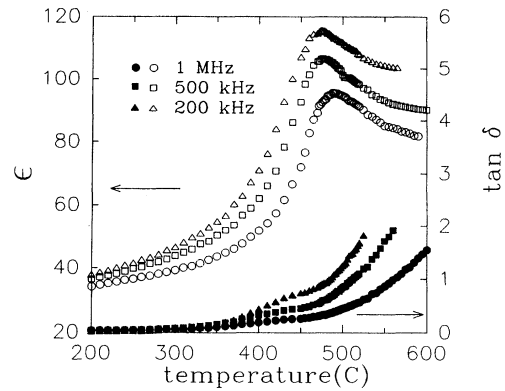


FIG. 8. Temperature dependence of  $\epsilon$  (empty symbols) and  $\tan\delta$  (filled symbols) in  $\text{PbTiO}_3$  with  $d_{\text{XRD}}=31$  nm for three different frequencies (200 kHz, 500 kHz, and 1 MHz).

( $c/a$ ) from 1.064 at  $d_{\text{XRD}}=148.0$  nm to 1.041 at  $d_{\text{XRD}}=23.4$  nm (Fig. 3). This is in accordance with the predictions of the “internal stress model” proposed by Buessem *et al.*<sup>16</sup> The model suggests that when a perfect single domain crystal with unconstrained surfaces makes a transition from the cubic paraelectric to the tetragonal ferroelectric state, the strain is developed fully and the crystal remains totally unstressed. When a fine-grained ceramic is cooled through  $T_c$ , each grain is subjected to a complex system of internal stresses which depend on the orientation of all the surrounding grains. The structural transformation accompanying the ferroelectric transition cannot develop fully due to such intergranular contacts, so that unrelieved strains remain within the grains (which cannot be relieved by the formation of 90° domains). Buessem *et al.* suggested that “the stress system would be of a type tending to suppress the spontaneous deformation and forcing the grain back towards the cubic state,” and argued that the stress system would consist of a combination of uniform mechanical compression along the  $c$  axis and tensions along both the  $a$  axes. Such a stress system would lead to a decrease in the  $T_c$ . The earlier data of Martirena and Burfoot<sup>4</sup> do not follow this trend because their study is limited to the 1–5  $\mu\text{m}$  range and, according to our data,  $c/a$  starts showing a strong dependence on particle size only below  $\approx 0.1$   $\mu\text{m}$ .

It is possible to estimate the critical size at which  $\text{PbTiO}_3$  transforms to the cubic (paraelectric) phase at room temperature. The  $c/a$  vs  $d_{\text{XRD}}$  data can be least-squares fitted with an equation of the form

$$y = y_\infty - C \exp[C(d_{\text{crit}} - x)], \quad (4)$$

with  $x \equiv d_{\text{XRD}}$ ,  $y \equiv c/a$ ,  $y_\infty \equiv 1.065$ , and  $C \equiv y_\infty - 1$ . The critical size  $d_{\text{crit}}$  is a fitting parameter. Eq. (4) satisfies the boundary conditions: (1)  $y \rightarrow y_\infty$  as  $x \rightarrow \infty$ , and (2)  $y \rightarrow 1$  as  $x \rightarrow d_{\text{crit}}$ . We find—by extrapolation—that  $c/a=1$  when  $d_{\text{crit}}=7.0$  nm. Note that the critical size (defined as the size at which  $T_c \rightarrow 0$  K) predicted by Zhong *et al.*<sup>17</sup> for  $\text{PbTiO}_3$ —using Landau’s phenomenological approach—is 4.2 nm.

The observed decrease of the tetragonal distortion with a reduction in the particle size appears to be a manifestation of

a more general phenomenon. We have recently shown<sup>18</sup> that in a large number of partially covalent oxides, the crystal lattice tends to transform into a structure of higher symmetry when the particle size becomes smaller. In certain systems (such as  $\text{Fe}_2\text{O}_3$  and  $\text{Al}_2\text{O}_3$ ), the size-induced distortion may be large enough to actually precipitate a crystallographic transition to a high-symmetry structure. In others (such as in the present case), there may be a gradual reduction in an asymmetry parameter (e.g.,  $c/a$ ) with decreasing size.

The lowering of the value of  $\varepsilon_{\text{max}}$  with a decrease in particle size can be attributed to a lower value of  $P_S$ , and to the pinning effect of the domain walls. When the grain size becomes comparable to the width of the domain walls, pinning points would develop inside the grains and the domain wall motion would be inhibited. The resulting reduction in the wall mobility would decrease the switching rate, thereby lowering  $\varepsilon_{\text{max}}$ .

### B. Size-induced diffused phase transition

Two of our measurements of  $T_c$  (dielectric and thermal) appear to indicate that the ferroelectric transition is suppressed in nanocrystalline  $\text{PbTiO}_3$  when  $d_{\text{XRD}}$  is reduced below  $\approx 30$  nm. This is in apparent contradiction with the structural measurements since the ferroelectric distortion corresponding to 30 nm is rather large ( $\approx 1.05$ ) and it does not actually vanish even in the finest particles studied. Note that in the isostructural  $\text{BaTiO}_3$ , a tetragonal distortion of only  $\approx 1.01$  is sufficient to stabilize the ferroelectric phase. We therefore suggest that the nonappearance of a peak in the dielectric and thermal response need not be construed as indicative of an absence of ferroelectric ordering.

The observed broadening of the dielectric as well as DSC peaks at the ferroelectric transition in nanocrystalline  $\text{PbTiO}_3$  is typical of “relaxor” materials which exhibit a diffused phase transition (DPT). DPT is usually characterized by the following signatures:<sup>19–24</sup> (a) a broadening in the maxima of the  $\varepsilon$ - $T$  curves, (b) a relatively large separation (in temperature) between the real and the imaginary parts of the dielectric permittivity maxima, (c) a deviation from Curie-Weiss law in the vicinity of  $T_c$ , (d) frequency-dependent character (dispersion) of both  $\varepsilon$  and  $\tan\delta$  in the transition region—implying a frequency dependence of the apparent  $T_c$ , (e) a gradual (rather than abrupt) decrease of the  $P_S$  across the apparent  $T_c$ , and (f) a difference in the value of  $T_c$  obtained from different physical measurements.

Our present study of  $\text{PbTiO}_3$  nanoparticles suggests that with a decrease in particle size: (a) the  $\varepsilon$ - $T$  peaks become broader, (b) the separation between the peaks in the  $\tan\delta$  vs  $T$  and  $\varepsilon$  vs  $T$  curves becomes larger with decreasing size, (c) there is an increasing deviation from the Curie-Weiss law (as shown later), (d) both  $\varepsilon$  vs  $T$  and  $\tan\delta$  vs  $T$  show a marked frequency dispersion, (e) the decrease in  $c/a$  (which is expected to scale with  $P_S$ ) as  $T \rightarrow T_c$  becomes more gradual in samples with smaller particle size, (f)  $T_c$  obtained from different measurements do not coincide (Table I), (g) with a decrease in frequency,  $T_c$  decreases and  $\varepsilon_{\text{max}}$  increases.

A quantitative estimate of the “diffuseness” of the ferroelectric phase transition in nanocrystalline  $\text{PbTiO}_3$  can be

made by fitting the portion of the  $\varepsilon$ - $T$  curve for  $T > T_{\text{max}}$  (where  $T_{\text{max}}$  corresponds to the peak in  $\varepsilon$ ) with the following equation:<sup>22</sup>

$$1/\varepsilon - 1/\varepsilon_{\text{max}} = C^{-1}(T - T_{\text{max}})^\gamma, \quad (5)$$

where  $C$  is a constant and the critical exponent  $\gamma = 1$  for a classical Curie-Weiss ferroelectric, and  $\gamma = 2$  for a system with a completely diffused transition—as predicted theoretically on the basis of a local compositional fluctuation model. For systems exhibiting intermediate degrees of diffuseness:  $1 < \gamma < 2$ . We determined the value of  $\gamma$  from the slope of a straight line fitted to the logarithmic plots of the reciprocal permittivity ( $1/\varepsilon - 1/\varepsilon_{\text{max}}$ ) measured at 1 MHz as a function of  $(T - T_{\text{max}})$ . We see from Table I that with a decrease in size, the ferroelectric transition becomes increasingly diffuse. For bulk  $\text{PbTiO}_3$ :  $\gamma = 1$ , whereas it is 1.5 for the sample with  $d_{\text{XRD}} = 31$  nm, below which the transition peak gets totally smeared.

DPT's were first recognized in perovskite solid solutions of the type  $A(P_{1-x}Q_x)\text{O}_3$ , in which, generally, there is no long range crystallographic ordering of the  $P$  and  $Q$  atoms. Local compositional fluctuations must therefore be present throughout the crystal; i.e., it would consist of microscopic domains of  $AP\text{O}_3$  and  $AQ\text{O}_3$ , having—in general—different values of  $T_c$ . (There could also be an intermixture of ferroelectric and paraelectric regions if only one of the constituent phases is ordered at the temperature of interest.) The scale of heterogeneity is believed<sup>23</sup> to be  $\sim 10$ – $20$  nm. The physical similarity between a solid solution and a nanocrystalline system now stands elucidated. A nanocrystalline ferroelectric with an average size of  $\sim 10$ – $20$  nm would consist of a collection of crystallites with varying sizes (due to the inherent size distribution) and, therefore, distinct  $T_c$ 's (due to the different  $c/a$  parameters associated with different sized particles). Since the variation of  $T_c$  with size is more conspicuous in smaller particles—the latter should exhibit a more diffused phase transition. A  $T_c$  distribution model had also been invoked<sup>4</sup> to explain the dielectric behavior of certain sintered ceramics, where a complicated stress distribution occurs due to the high compaction. In the comparatively loosely aggregated nanocrystalline material studied by us, the observed strain (and the  $T_c$ ) appears to depend directly on the particle size.

We should point out that, technically, a sharp phase transition (i.e., a singularity in the free energy) can occur only in the thermodynamical ( $N \rightarrow \infty$ ) limit. In a finite system, the phase transition gets smeared and shifted.<sup>25</sup> In a compact particle with nonfractal surfaces, and a volume  $\propto N$ , the extent of the smearing and shifting of the phase transition are given, respectively, by

$$\Delta T \propto N^{-1/d} \quad (6a)$$

and

$$[T_c(N) - T_c(\infty)] \propto N^{-1/d}, \quad (6b)$$

where  $d$  = spatial dimensionality. This type of size-induced smearing is distinct from that discussed above, and could become significant at even lower sizes.

## V. CONCLUSIONS

Our study of the ferroelectric phase transition in a small solids ensemble of  $\text{PbTiO}_3$  suggests that the following sequence of events occurs with a decrease in the average (coherently diffracting) domain size.

(i) Below a size of  $\approx 0.1 \mu\text{m}$ , the tetragonal distortion ( $c/a$ ) starts decreasing monotonically ( $\sim 1 - e^{-d}$ ). This behavior is not only in accordance with the model proposed by Buessem *et al.* but appears to be a general consequence of the decrease in particle size in a large class of compounds. The decrease in  $c/a$  is accompanied by a decrease in the  $T_c$  by about  $20^\circ\text{C}$  corresponding to a change in  $d_{\text{XRD}}$  from  $\approx 80$  to  $\approx 30$  nm.

(ii) A decrease in the particle size makes the ferroelectric transition increasingly diffuse. The “diffuseness coefficient” ( $\gamma$ ) increases from 1.00 (perfect Curie-Weiss behavior) for  $\approx 80$  nm particles to 1.50 for  $\approx 30$  nm ones. Accordingly, the dielectric and thermal transitions at  $T_c$  become progressively broader and shallower before they disappear altogether at 26 nm. Since  $c/a$  and hence the  $T_c$  depend strongly on the particle size, the above behavior would arise from the almost inevitable existence of a particle size distribution about the mean value.

(iii)  $\text{PbTiO}_3$  nanoparticles with  $d_{\text{XRD}} = 26$  nm do not ex-

hibit any peak corresponding to the ferroelectric transition in DSC and dielectric measurements. However, we believe that these particles *are* ferroelectrically ordered since the tetragonal distortion (though less than the bulk value) is still comparatively high in particles of this size.

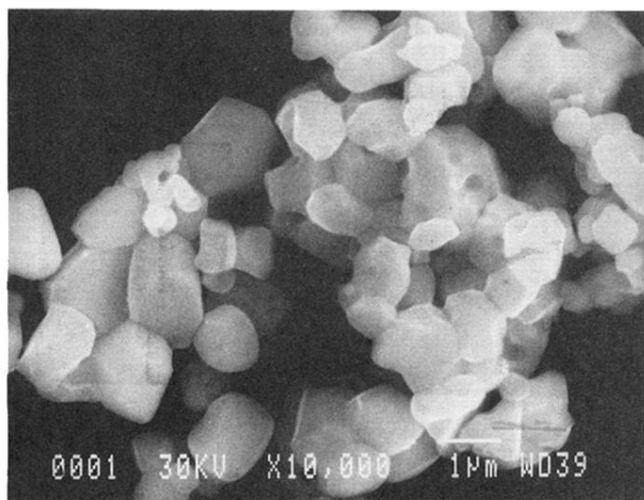
(iv) The tetragonal distortion (extrapolated) approaches unity when  $d_{\text{XRD}} \cong 7$  nm. This, therefore, should be considered as the “critical size” at which a ferroelectric  $\leftrightarrow$  paraelectric transition takes place at room temperature in  $\text{PbTiO}_3$ .

The actual values of the particle size for which there is a crossover from one of the above types of behavior to the next would depend on the particle size distribution as well as on the nature of the intragranular contacts and the resulting stresses. Thus, we may expect some differences (in samples of the same compound) due to different methods of synthesis and compaction.

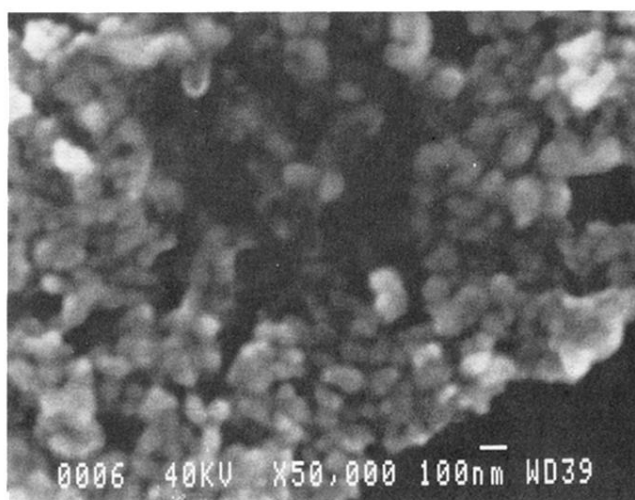
## ACKNOWLEDGMENTS

It is a pleasure to acknowledge the support and encouragement received from Professor R. Vijayaraghavan. We thank Mr. A. V. Gurjar and Mr. R. M. Wankar for their skillful help in some experiments, and Mr. S. C. Purandare for providing the SEM observations.

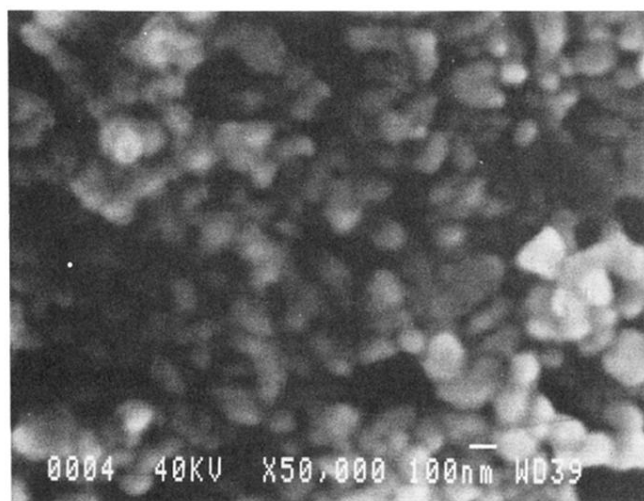
- 
- <sup>1</sup>M. Anliker, H. R. Brugger, and W. Känzig, *Helv. Phys. Acta* **27**, 99 (1954).  
<sup>2</sup>W. Känzig, *Phys. Rev.* **98**, 549 (1955).  
<sup>3</sup>K. Okazaki and K. Nagata, *J. Am. Ceram. Soc.* **56**, 82 (1973).  
<sup>4</sup>H. T. Martirena and J. C. Burfoot, *J. Phys. C* **7**, 3182 (1974).  
<sup>5</sup>M. R. Srinivasan, M. S. Multani, P. Ayyub, and R. Vijayaraghavan, *Ferroelectrics* **51**, 137 (1983).  
<sup>6</sup>T. Kanata, T. Yoshikawa, and K. Kubota, *Solid State Commun.* **62**, 765 (1987).  
<sup>7</sup>K. Uchino, E. Sadanaga, and T. Hirose, *J. Am. Ceram. Soc.* **72**, 1555 (1989).  
<sup>8</sup>K. Ishikawa, K. Yoshikawa, and N. Okada, *Phys. Rev. B* **37**, 5852 (1988).  
<sup>9</sup>G. Burns and B. A. Scott, *Phys. Rev. Lett.* **25**, 167 (1970); *Phys. Rev. B* **7**, 3088 (1973).  
<sup>10</sup>W. L. Zhong, B. Jiang, P. L. Zhang, J. M. Ma, H. M. Cheng, Z. H. Yang, and L. X. Li, *J. Phys. Condens. Matter* **5**, 2619 (1993).  
<sup>11</sup>A. J. C. Wilson, *Proc. Phys. Soc. London* **80**, 286 (1962).  
<sup>12</sup>B. E. Warren, *X-ray Diffraction* (Addison-Wesley, New York, 1969).  
<sup>13</sup>T. R. Anantharaman and J. W. Christian, *Acta Crystallogr.* **9**, 479 (1956).  
<sup>14</sup>W. A. Rachinger, *J. Sci. Instrum.* **25**, 254 (1948).  
<sup>15</sup>T. Allen, *Particle Size Measurement* (Chapman and Hall, London, 1975), p. 358.  
<sup>16</sup>W. R. Buessem, L. E. Cross, and A. K. Goswami, *J. Am. Ceram. Soc.* **49**, 33 (1966).  
<sup>17</sup>W. L. Zhong, Y. G. Wang, P. L. Zhang, and B. D. Qu, *Phys. Rev. B* **50**, 698 (1994).  
<sup>18</sup>P. Ayyub, V. R. Palkar, S. Chattopadhyay, and M. S. Multani, *Phys. Rev. B* **51**, 6135 (1995).  
<sup>19</sup>G. Smolenskii, *J. Phys. Soc. Jpn. Suppl.* **28**, 26 (1970).  
<sup>20</sup>C. G. F. Stenger and A. G. Burggraaf, *J. Phys. Chem. Solids* **41**, 25 (1980).  
<sup>21</sup>W. K. Choo and M. H. Lee, *J. Appl. Phys.* **53**, 7355 (1982).  
<sup>22</sup>K. Uchino and S. Nomura, *Ferroelectrics Lett.* **44**, 55 (1982).  
<sup>23</sup>L. E. Cross, *Ferroelectrics* **76**, 241 (1987).  
<sup>24</sup>V. S. Tiwari and D. Pandey, *J. Am. Ceram. Soc.* **77**, 1819 (1994).  
<sup>25</sup>K. Binder, *Ferroelectrics* **73**, 43 (1987).



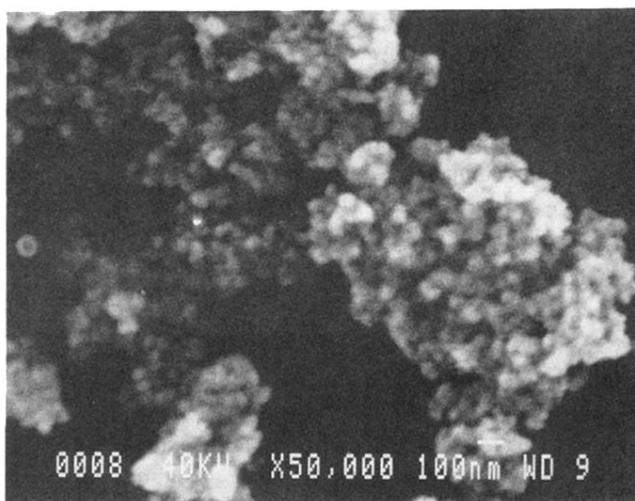
(a)



(c)



(b)



(d)

FIG. 1. SEM images of (a) bulk (Johnson Matthey, Puratronic grade)  $\text{PbTiO}_3$ ,  $\text{ESD}=1.77\ \mu\text{m}$  ( $\times 10\ 000$ ), and three typical samples of  $\text{PbTiO}_3$  produced by coprecipitation with (b)  $\text{ESD}=111\ \text{nm}$  ( $\times 50\ 000$ ), (c)  $\text{ESD}=83.5\ \text{nm}$  ( $\times 50\ 000$ ), and (d)  $\text{ESD}=43.5\ \text{nm}$  ( $\times 50\ 000$ ).